

Design of Hybrid Precoder for mm-Wave MIMO System Based on Generalized Triangular Decomposition Method

Sammaiah Thurpati, and P Muthuchidambaranathan

Abstract—Hybrid precoding techniques are lately involved a lot of interest for millimeter-wave (mmWave) massive MIMO systems is due to the cost and power consumption advantages they provide. However, existing hybrid precoding based on the singular value decomposition (SVD) necessitates a difficult bit allocation to fit the varying signal-to-noise ratios (SNRs) of altered sub-channels. In this paper, we propose a generalized triangular decomposition (GTD)-based hybrid precoding to avoid the complicated bit allocation. The development of analog and digital precoders is the reason for the high level of design complexity in analog precoder architecture, which is based on the OMP algorithm, is very non-convex, and so has a high level of complexity. As a result, we suggest using the GTD method to construct hybrid precoding for mmWave mMIMO systems. Simulated studies as various system configurations are used to examine the proposed design. In addition, the archived findings are compared to a hybrid precoding approach in the classic OMP algorithm. The proposed Matrix Decomposition's simulation results of signal-to-noise ratio vs spectral efficiencies

Keywords—millimeter-wave (mmWave); SVD; GTD.; Hybrid precoding; massive MIMO

I. INTRODUCTION

mMIMO is a key technology for 5G systems to improve spectrum utilization and system capacity. The M-MIMO system uses hybrid precoding technology to improve spectral efficiency (SE) and eliminate inter-signal interference [1]. This problem is considered to be one of the biggest challenges for dense networks in the future. The 5G network aims to current SE, quality of service (QoS), and higher system capacity such as the use of a wider spectrum. Future networks will demand faster data rates and broader bandwidths to serve heavy data traffic, hence the surviving range below 6 GHz will no longer serve. Therefore, recently as considered mmWave frequencies have a practical solution to bandwidth tricky [2]. The millimeter-wave frequency between 30 GHz to 300 GHz will become the spectrum resource on upcoming wireless networks because the use of these abundant and available frequencies to achieve higher data rates has great potential. Due to these characteristics, communication signals exhibit more severe path loss than existing systems operating in the frequency band below 6 GHz. To mitigate these problems,

Authors are with Department of Electronics and Communication Engineering, National Institute of Technology, Tiruchirappalli, India (e-mail:sammaiah_404@yahoo.com, muthuc@nitt.edu).

multiple antennas are usually considered at the station [3]. The combination of millimeter-wave communication system and millimeter-wave communication system millimeter-wave frequency and massive MIMO system. However, it is still necessary to use precoding methods for directional beamforming to improve system performance .

Digital precoding is expensive to implement in millimeter-wave communication systems. As a result, hybrid precoding is mixes analog and digital precoding and preferable alternative. In [1], spatial sparsity is used to reconstruct the hybrid precoding problem, and the OMP algorithm is projected to tackle the problem. A threshold OMP algorithm is performance similar to the optimal and better than the OMP method is proposed by developing a suitable threshold [4], [5], [6]. Even though the OMP algorithm has good performance, it has a relatively high level of complexity. As a result, a high-performance real-time precoding method built on singular value decomposition is being investigated. In the hybrid precoding problem was initially framed as matrix factorization tricky, and then the OMP technique was used to discover near-optimal analog and digital precoders. The authors of [7], [8] used the formalism presented in the designed hybrid precoders using a manifold-based alternating minimization approach. The hybrid precoding techniques are Low complexity based on matrix factorization was introduced and evaluated in references [9], [10], [11], [12].

For example, mmWave communication has reached gigabit data rates per second in wireless indoor systems and outdoor systems . Recently, improvements in millimeter-wave hardware and the convenience of frequencies have stimulated the cellular industry to consider millimeter waves on access connections in cellular outdoor systems [3], [14]. A key difference in millimeter-wave communications is that compared to most current wireless systems, the carrier frequency is increased by 10 times, which means that the free space path-loss of millimeter-wave signals will increase by several orders of magnitude [19], [20]. However, an interesting balance characteristic in millimeter-wave systems is that the reduction in wavelength brands it possible to package a significant number of antenna elements into a



small size. In addition, huge arrays can allow precoding of multiple data streams, which can improve spectral efficiency and bring the system closer to capacity [21], [22].

In this investigation, considering the above situation, a hybrid precoding system using the GTD method was considered for the massive mmWave MIMO system [15], [16], [17]. The designer of the performance precoder has been thoroughly studied through a series of simulation studies. Furthermore, the suggested hybrid precoder is associated to a hybrid precoder based on the OMP method that was described earlier. The study of evaluation and simulation confirmed based on the standard OMP algorithm, the suggested hybrid precoder is better than the hybrid precoder over the SNR range. The respite of this article is systematized as follows. Section 2 covers the system model and channel model. Section 3 explains the design approaches. Section 4 and 5 introduce the Single User mm-Wave Channel on Spatially Sparse Precoding the millimeter-wave channel model and system, and the basic knowledge of the GTD method. In Section 6, the numerical results and simulated results of the proposed design are presented. Finally, section 7 concludes the work.

par

II. SYSTEM MODEL

The hybrid precoding framework of the hybrid connection structure in the mmWave mMIMO system is in Fig. 1. The antenna communicates N_s as data streams, the receiver and transmitter are equipped with N_r & N_t antennas. At the transmitter, the total RF link is divided into D sub-arrays. Each sub-array S has RF links, so there are a total of SD RF links and DN transmitting antennas, namely $N_{RF} = SD, N_t = DN$. Each sub-array S is connected to RF links. To facilitate the hybrid precoding performance is estimated. At the receiving end and the transmitting end, the number of radiofrequency links satisfies $N_s \leq SD \leq N_t$, and $N_s \leq SD \leq N_r$ respectively.

The signal vector is received $y = [y_1, y_2, y_3, \dots, y_{N_r}]^T$

$$y = \sqrt{\rho} H F_{RF} F_{BB} + n \quad (1)$$

where, F_{BB} means $SD \times N_s$ order digital precoding matrix, F_{RF} means $N_t \times SD$ order analog precoding matrix, ρ means average received power, $H \in C^{(N_r N_t)}$ means channel matrix, s means $N_s \times 1$ order Transmit signal matrix, and meet $E[ss^H] = \frac{1}{N_s} I_{N_s}$ represents the hybrid precoding matrix, meet the total transmit power limit $\|F_{RF} F_{BB}\|_F^2 \leq N_s, n \sim CN(0, \sigma_n^2)$ represents the channel noise vector. Considering the sparse appearances of the millimeter-wave channel system, the article uses the S-V (Saleh-Valenzuela) model [1]. In wireless channels, the parameters of the transmission path are SV-based channel model is a parameterized multipath channel model established. The parameterized channel model is more direct and more direct than estimating each element in the channel matrix for a large-scale antenna array system. A more efficient way, especially for millimeter-wave channels, because

the higher path loss in millimeter-wave transmission severely restricts the number of paths transmitted in the channel, so the parametric channel model only needs to know less path information to determine the millimeter-wave model.

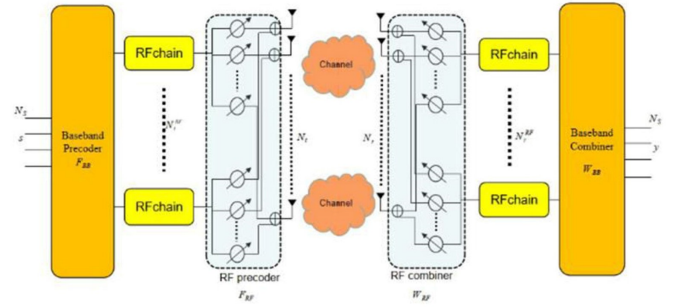


Fig. 1. Hybrid precoding framework in MM-MIMO system

A. Channel Model

The widely used Saleh-Valenzuela (SV) channel model for mmWave communication, where the H of the channel matrix is.

$$H = \sqrt{\frac{N_t N_r}{G}} \beta_o a_r(\phi_o^r) a_t^H(\phi_o^t) + \sum \beta_i a_t^H(\phi_i^t) a_r(\phi_i^r) \quad (2)$$

where $\beta_o a_r(\phi_o^r) a_t^H(\phi_o^t)$ is the Line of Sight (LoS) component with β_o presenting the complex gain, ϕ_o^r presenting the angle of arrival (AoA) at the user, ϕ_o^t presenting the angle of departure (AoD) at the BS, and $\beta_i a_r(\phi_i^r) a_t^H(\phi_i^t)$ denotes the i^{th} non-Line of Sight (NLoS) component. In $a_r(\phi_i^r)$ and $a_t(\phi_i^t)$ denote the array response vectors at the user, G is the total number of paths and the BS is ULA with elements N [8].

$$a_{ULA}(\phi) = \frac{1}{\sqrt{N}} [1, e^{dsin(\phi)j\frac{2\pi}{\lambda}}, \dots, e^{dsin(\phi)j(N-1)\frac{2\pi}{\lambda}}]^T \quad (3)$$

Where the antenna spacing is d and λ denotes the wavelength. Due to mm-wave propagation is limited scattering characteristics, the channel matrix rank H is bigger than the number of antennas. Therefore, the hybrid precoding structure is the near-optimal performance as an influence to data a slight number of RF chains to be achieved.

III. DESIGN APPROACH

A. Problem Formulation

The main objective of this work is to improve the SE based on various matrix factorization methods. By the proposed system and channel model in section II. When the transmitted signal obeys Gaussian distribution, the SE of the hybrid connection structure is

$$R = \log_2 \left(|I_{N_s} + \frac{\rho}{N_s} R_n^{-1} W_{BB}^H W_{RF}^H H F_{RF} F_{BB} F_{BB}^H F_{RF}^H H^H W_{RF} W_{BB}| \right) \quad (4)$$

This proposed work takes the maximization of formula (4) as the optimization goal to design the optimal hybrid precoding matrix $F_{RF}F_{BB}$, through matrix decomposition, the GTD and the OMP method are used to optimize the design of the digital and analog precoding matrix F_{BB}, F_{RF} to make F_{BB}, F_{RF} as close to the optimal F as the possible matrix. According to the idea of continuous interference elimination, the optimal hybrid precoding matrix F^{opt} with limited power and no constant modulus constraint in the analog part is obtained [6].

We want to create ($F_{RF}F_{BB}$) hybrid mmWave precoders that maximize the expression of SE (4). To make transceiver design easier, the joint receiver-transmitter optimization problem is temporarily decoupled so that the design of $F_{RF}F_{BB}$ can be concentrated. As a result, rather than increasing spectral efficiency, the $F_{RF}F_{BB}$ is designed to exploit the information acquired via Gaussian signaling over the mm-Wave channel.

$$\mathcal{I}(F_{RF}, F_{BB}) = \log_2(I_{N_t} + \frac{\rho}{N_s \sigma_n^2} H F_{RF} F_{BB} F_{BB}^H F_{RF}^H H^H) \quad (5)$$

We note here above equation $F = F_{RF}F_{BB}$, that conceptualizing receiver process and concentrating on shared information rather than the SE expression in (4) the optimal adjacent-neighbor decoding of the receiver can conduct on well amount to affected based on the y is the N_r -dimensional received signal. The precoder optimization challenge might be described as follows as we move on with the design of $F_{RF}F_{BB}$:

$$(F_{RF}^{opt}, F_{BB}^{opt}) = \arg \max_{F_{RF}F_{BB}} \log_2(I_{N_t} + \frac{\rho}{N_s \sigma_n^2} H F_{RF} F_{BB} F_{BB}^H F_{RF}^H H^H) \quad (6)$$

$$\text{s.t. } F_{RF} \in \mathcal{F}_{RF},$$

$$\|F_{RF}F_{BB}\|_F^2 = N_s$$

B. Singular Value Decomposition based Digital Precoding

The mutual information is obtained by the hybrid precoders $F_{RF}F_{BB}$ and rephrasing (5) as to the “distance” among $F_{RF}F_{BB}$ and F_{opt} precoder of the channel is optimally unconstrained. This, describe the channel’s $H = U\Sigma V^H$ where Σ is a $\text{rank}(H) \times \text{rank}(H)$ diagonal matrix of singular values obvious as reducing order, U is a single $N_r \times \text{rank}(H)$ unitary matrix and V is a $N_t \times \text{rank}(H)$ unique matrix. Taking the SVD of H and usual mathematical operation, (5) can be modified as

$$\mathcal{I}(F_{RF}, F_{BB}) = \log_2(|\mathbf{I} + \frac{\rho}{\sigma_n^2 N_s} \Sigma^2 \mathbf{V}^* F_{RF} F_{BB} F_{BB}^* F_{RF}^* \mathbf{V}|) \quad (7)$$

Further, define the following two matrices partitions Σ and \mathbf{V} as

$$\Sigma = \begin{bmatrix} \Sigma_1 & 0 \\ 0 & \Sigma_2 \end{bmatrix}, \mathbf{V} = [\mathbf{V}_1 \quad \mathbf{V}_2] \quad (8)$$

where the dimension of Σ_1 is $N_s \times N_s$ and the dimension of \mathbf{V}_1 is $N_s \times N_t$, the optimal unconstrained is the H as given by $F_{opt} = V_1$. Additionally, the \mathbf{V}_1 precoder is to be $F_{RF}F_{BB}$ with $F_{RF} \in \mathcal{F}_{RF}$. As a result, the mmWave construction of attention cannot be achieved. If $F_{BB}F_{RF}$ can be finished adequately “close” V_1 . however, the information is shared resulting from $F_{BB}F_{RF}$ and F_{opt} is similar.

Approximation 1: The mmWave system parameters ($N_t, N_r, N_t^{RF}, N_r^{RF}$), in addition to the propagation channel of the mm-Wave (N_{cl}, N_{ray}, \dots), and $F_{BB}F_{RF}$ can be made sufficiently “close” to the optimal unitary precoder $F_{opt} = V_1$. The following two equivalent approximations:

- $\mathbf{I}_{N_s} - \mathbf{V}_1^H F_{RF} F_{BB} F_{BB}^H F_{RF}^* \mathbf{V}_1$. Its eigenvalues of the matrix are minor. In the situation of mmWave precoding, is constantly stated as $\mathbf{V}_1^H F_{RF} F_{BB} \approx \mathbf{I}_{N_s}$.
- $\mathbf{V}_2^* F_{RF} F_{BB} \approx 0$. Its singular values of the matrix ;

The high-resolution estimate of the approximate is similar, which assumes that codebooks are large enough to include code words that are the ideal quantized precoder is sufficiently close to simplifying the study of limited feedback MIMO systems. This approximation is likely to be close in the case of mmWave precoding in systems of attention such as: (i) Number of antennas N_t is significant.

- (ii) A slew of transmission chains $N_s < N_t^{RF} \leq N_t$, and
- (iii) \mathbf{H} is a correlated matrix.

We use and rewrite (6) and the further following is

$$\begin{aligned} & \mathbf{V}^H F_{RF} F_{BB} F_{BB}^H F_{RF}^* \mathbf{V} \text{ as} \\ & \mathbf{V}^H F_{RF} F_{BB} F_{BB}^H F_{RF}^* \mathbf{V} \\ & = \begin{bmatrix} \mathbf{V}_1^H F_{RF} F_{BB} F_{BB}^H F_{RF}^* \mathbf{V}_1, & \mathbf{V}_1^H F_{RF} F_{BB} F_{BB}^H F_{RF}^* \mathbf{V}_2 \\ \mathbf{V}_2^H F_{RF} F_{BB} F_{BB}^H F_{RF}^* \mathbf{V}_1, & \mathbf{V}_2^H F_{RF} F_{BB} F_{BB}^H F_{RF}^* \mathbf{V}_2 \end{bmatrix} \\ & = \begin{bmatrix} \mathbf{Q}_{11} & \mathbf{Q}_{12} \\ \mathbf{Q}_{21} & \mathbf{Q}_{22} \end{bmatrix} \quad (9) \end{aligned}$$

As a result, we can approximate the information obtained by $F_{RF}F_{BB}$ as

$$\begin{aligned} \mathcal{I}(F_{RF}, F_{BB}) & = \log_2(|\mathbf{I} + \frac{\rho}{\sigma_n^2 N_s} \Sigma^2 \mathbf{V}^H F_{RF} F_{BB} F_{BB}^H F_{RF}^* \mathbf{V}|) \\ & = \log_2(|\mathbf{I} + \frac{\rho}{\sigma_n^2 N_s} \begin{bmatrix} \Sigma_1^2 & 0 \\ 0 & \Sigma_2^2 \end{bmatrix} \begin{bmatrix} \mathbf{Q}_{11} & \mathbf{Q}_{12} \\ \mathbf{Q}_{21} & \mathbf{Q}_{22} \end{bmatrix}|) \\ & \text{(a)} \\ & = \log_2(|\mathbf{I}_{N_s} + \frac{\rho}{\sigma_n^2 N_s} \Sigma_1^2 \mathbf{Q}_{11}|) + \log_2(|\mathbf{I} + \frac{\rho}{\sigma_n^2 N_s} \Sigma_2^2 \mathbf{Q}_{22} - \frac{\rho^2}{\sigma_n^4 N_s^2} \Sigma_2^2 \mathbf{Q}_{21} (\mathbf{I}_{N_s} + \frac{\rho}{\sigma_n^2 N_s} \Sigma_1^2 \mathbf{Q}_{11})^{-1} \Sigma_1^2 \mathbf{Q}_{12}|) \\ & \text{(b)} \approx \log_2(|\mathbf{I}_{N_s} + \frac{\rho}{\sigma_n^2 N_s} \Sigma_1^2 \mathbf{V}_1^* F_{RF} F_{BB} F_{BB}^* F_{RF}^* \mathbf{V}_1|) \quad (10) \end{aligned}$$

where (a) is the consequence of applying the S-V accompaniment identity to matrix determinants, and (b) is the result of applying Approximation 1 which states that

\mathbf{Q}_{12} , \mathbf{Q}_{21} and \mathbf{Q}_{21} are close to 0. By putting down mutual information (12).

$$\begin{aligned}
 & \text{(a)} \\
 I(\mathbf{F}_{RF}, \mathbf{F}_{BB}) & \approx \log_2(|\mathbf{I}_{N_s} + \frac{\rho}{\sigma_n^2 N_s} \Sigma_1^2|) + \log_2(|\mathbf{I}_{N_s} - (\mathbf{I}_{N_s} + \frac{\rho}{\sigma_n^2 N_s} \Sigma_1^2)^{-1} \times \frac{\rho}{\sigma_n^2 N_s} \Sigma_1^2 (\mathbf{I}_{N_s} - \mathbf{V}_1^H \mathbf{F}_{RF} \mathbf{F}_{BB} \mathbf{F}_{BB}^H \mathbf{F}_{RF}^H \mathbf{V}_1)|) \\
 & \text{(b)} \\
 & \approx \log_2(|\mathbf{I}_{N_s} + \frac{\rho}{\sigma_n^2 N_s} \Sigma_1^2|) - \text{tr}((\mathbf{I}_{N_s} + \frac{\rho}{\sigma_n^2 N_s} \Sigma_1^2)^{-1} \times \frac{\rho}{\sigma_n^2 N_s} \Sigma_1^2 (\mathbf{I}_{N_s} - \mathbf{V}_1^H \mathbf{F}_{RF} \mathbf{F}_{BB} \mathbf{F}_{BB}^H \mathbf{F}_{RF}^H \mathbf{V}_1)) \\
 & \text{(c)} \\
 & \approx \log_2(|\mathbf{I}_{N_s} + \frac{\rho}{\sigma_n^2 N_s}|) - \text{tr}(\mathbf{I}_{N_s} - \mathbf{V}_1^H \mathbf{F}_{RF} \mathbf{F}_{BB} \mathbf{F}_{BB}^H \mathbf{F}_{RF}^H \mathbf{V}_1) \\
 & \approx \log_2(|\mathbf{I}_{N_s} + \frac{\rho}{\sigma_n^2 N_s}|) - (N_s - \|\mathbf{V}_1^H \mathbf{F}_{RF} \mathbf{F}_{BB} \mathbf{F}_{BB}^H \mathbf{F}_{RF}^H \mathbf{V}_1\|_F^2) \quad (12)
 \end{aligned}$$

Approximation 1, $X = (\mathbf{I}_{N_s} + \frac{\rho}{N_s \sigma_n^2} \Sigma_1^2)^{-1} \frac{\rho}{N_s \sigma_n^2} \Sigma_1^2 (\mathbf{I}_{N_s} - \mathbf{V}_1^H \mathbf{F}_{RF} \mathbf{F}_{BB} \mathbf{F}_{BB}^H \mathbf{F}_{RF}^H \mathbf{V}_1)$ is the eigenvalues of the matrix are a subsequent approximation $\log_2 |\mathbf{I}_{N_s} - \log_2(1 - \text{tr}(X))| \approx X \approx -\text{tr}(X)$. Finally (c) tracks from espousing a high SNR estimate that $(I + \frac{\rho}{N_s \sigma_n^2} \Sigma_1^2)^{-1} \frac{\rho}{N_s \sigma_n^2} \Sigma_1^2 \approx \mathbf{I}_{N_s}$ and the final results (10). We sign that the joint data attained by the optimal precoder $F_{opt} = \mathbf{V}_1$ is the first term in (12) and the need of $I(F_{BB}, F_{RF})$ on the hybrid precoder F_{BB}, F_{RF} .

IV. THE SINGLE USER MM-WAVE CHANNEL ON SPATIALLY SPARSE PRECODING

The Grassmann manifold, we can see the second term in (11) and (12) is nothing more than the formed to the two points $F_{opt} = \mathbf{V}_1$ and $F_{RF} F_{BB}$ is made perfectly unitary. To substitute the chordal distance with the Euclidean distance $\|F_{opt} - F_{RF} F_{BB}\|_F$ to use the manifold's locally Euclidean attribute. Because Approximation 1 states that as a result, by minimizing instead of, that roughly maximize $I(F)$ can be found by instead minimizing the near-optimal hybrid precoders $\|F_{opt} - F_{RF} F_{BB}\|_F$.

Approximation 1 concludes that $\|\mathbf{V}_1^H F_{RF} F_{BB}\|_F^2$, and accordingly (12), is roughly exploited by instead maximizing $\text{tr}(\mathbf{V}_1^H F)$. Since the equivalent of exploiting $\text{tr}(\mathbf{V}_1^H F_{RF} F_{BB})$ is minimizing $F_{opt} - F_{RF} F_{BB}\|_F$, The revised of the precoder design problem as $(F_{RF}^{opt}, F_{BB}^{opt}) = \arg \min_{F_{RF}, F_{BB}} \|F_{opt} - F_{RF} F_{BB}\|_F$

$$s.t. F_{RF} \in \mathcal{F}_{RF} \quad (13)$$

$$\|F_{RF} F_{BB}\|_F^2 = N_s$$

which be potted as discovery the forecast of hybrid precoders in the F_{opt} of the form $F_{RF} F_{BB}$ with $F_{RF} \in \mathcal{F}_{RF}$. This forecast is well-defined concerning the standard Frobenius norm $\|\cdot\|_F^2$ [13]–[14]. As a result of utilizing H's structure, we discover and develop the near-optimal field. By additional restricting the set of vectors, F_{RF} is the form $a_t(\phi_{il}^t, \theta_{il}^t)$ and solving $(F_{RF}^{opt}, F_{BB}^{opt}) = \arg \min \|F_{opt} - F_{RF} F_{BB}\|_F$

$$s.t. F_{RF}^{(i)} \in \{a_t(\phi_{il}^t, \theta_{il}^t) | N_{cl} \geq i \geq 1, N_{ray} \geq l \geq 1\} \quad (14)$$

$$\|F_{RF} F_{BB}\|_F^2 = N_s \quad (15)$$

It entails using the basis vectors $a_t(\phi_{il}^t, \theta_{il}^t)$ to find the representation of optimum low-dimensional is F_{opt} . The precoding challenge entails choosing the "best" N_t^{RF} array response vectors $a_t(\phi_{il}^t, \theta_{il}^t)$ and determining the appropriate baseband combination for them. Finally, we notice that the F_{RF}^t can be directly integrated the identical issue.

V. HYBRID PRECODING BASED ON GTD

The operation of SVD yields $H = U \Sigma V^H$, The rank K of channel matrix is $H \in C^{M \times N}$, $V \in C^{K \times M}$ and $U \in C^{K \times N}$ is semi-unitary matrices. The positive singular values of the diagonal matrix $\Sigma = \text{diag}\{\varpi\}$ involve in downward order i.e. $(\sigma_1 \geq \sigma_2 \geq \dots \geq \sigma_K)$, and $\varpi = [\sigma_1, \sigma_2, \dots, \sigma_K]^H$. Conferring to the GTD technique [24], The semi-unitary matrices are $H = QRP^H$, $P = C^{K \times M}$ and $Q = C^{K \times N}$. The upper triangular matrix $R = C^{K \times K}$ that satisfies $\text{diag}\{R\} = r$ condition where $r = [r_1, r_2, \dots, r_K]^H$. The Weyls multiplicative majored conditions are realized in GTD [22], [?]

$$\prod_{i=1}^K |r_i| \leq \prod_{i=1}^K |\sigma_i| \text{ and } \prod_{i=1}^{K-1} |r_i| \leq \prod_{i=1}^{K-1} |\sigma_i| \quad (16)$$

The workspace i for entire $i = 1, 2, \dots, K$. Is an initial condition with the assumption of $R^{(i)} = \Sigma$ and $i = 1$ in the GTD process. For the consistent $Q(i) \in C^{K \times K}$ & $P(i) \in C^{K \times K}$ at i th iteration, is convert $(i, i)^{th}$, r_i to $R^{(i+1)} = R^{(i)} P^{(i)} (Q^{(i)})^H$. In addition to getting the matrix Π and $\Pi^H R^{(K)} \Pi$ is symmetrical variation manner practical on $(i+1, i+1)$, $R^{(i)}$ moves the diagonal fundamentals of $R_{p,p}^{(i)}$ and $R_{q,q}^{(i)}$ to (i, i) .

$$p = \arg \min_{j=1, \dots, K} \{R_{j,j}^{(i)} : R_{j,j}^{(i)} \geq r_i\} \quad (17)$$

$$q = \arg \min_{j=1, \dots, K, j \neq p} \{R_{j,j}^{(i)} : R_{j,j}^{(i)} \leq r_i\} \quad (18)$$

To determine the communication to the workspace i of $\tilde{R}^{(j)} = \text{diag}\{\sigma_1, \sigma_2\}$, $\Pi^H R^{(j)} \Pi$. Subsequently, G_1 and G_2 are the identity matrices, which assist as rotation matrices, substituted by \tilde{G}_1 and \tilde{G}_2 and the following

$$\tilde{G}_1 = \begin{bmatrix} \mathbf{c} & \mathbf{s} \\ -\mathbf{s} & \mathbf{c} \end{bmatrix}, \tilde{G}_2 = \begin{bmatrix} \mathbf{c}\sigma_1 & \mathbf{s}\sigma_2 \\ -\mathbf{s}\sigma_2 & \mathbf{c}\sigma_1 \end{bmatrix}^H \quad (19)$$

Where $s = \sin\theta$, $c = \cos\theta$ and $\theta = \tan^{-1}\{\sqrt{(\sigma_1^2 - r_i^2)/(r_i^2 - \sigma_2^2)}\}$ i.e $|\sigma_2| \leq |r_i| \leq |\sigma_1|$ condition as satisfied. Now to obtain \tilde{G}_1 and $(\tilde{G}_2)^H$ matrices are $\tilde{R}^{(i)}$ multiplied $\begin{bmatrix} \mathbf{r}_i & \mathbf{x} \\ \mathbf{0} & \mathbf{y} \end{bmatrix} = (\tilde{G}_2)^H \tilde{R}^{(i)} \tilde{G}_1$

$$x = (\sigma_2^2 - \sigma_1^2)/r_i, y = \sigma_1 \sigma_2 / r_i \quad (20)$$

Finally, $(Q^i)^H P^{(i)} R^{(i)} = R^{(i+1)}$ is calculated where in $Q^i = \Pi G_2$ and $P^{(k)} = \Pi G_1$. These steps will be frequent till counter stretched to extreme value.

$$R = (Q^{(K-1)})^H = R^{(K)} \dots (Q^1)^H \Sigma P^1 \dots P^{(K-1)} \quad (21)$$

$$Q = U Q^{(1)} \dots Q^{(K-1)} \quad (22)$$

$$P = P^{(K-1)} \dots V P^{(1)} \quad (23)$$

A. GTD based Precoding Design

In mm-Wave mMIMO systems, the design of hybrid precoding techniques is presented in this subsection. Precoders and combiners have two distinct design problems that can be investigated separately. When slight variations between them are neglected, these design challenges might be considered equivalent design transactions [18]. The associated precoder design challenge can be phrased similarly to that reported.

$$\tilde{F}_{BB}^{opt} = \arg \min_{\tilde{F}_{BB}} \|F_{opt} - D_t \tilde{F}_{BB}\|_F$$

$$s.t. \|\text{diag}(\tilde{F}_{BB} \tilde{F}_{BB}^H)\|_0 = N_t^{RF} \quad (24)$$

$$\|D_t \tilde{F}_{BB}\|_F^2 = N_s$$

Where $D_t = [a_t(\theta_1^t, \phi_1^t), a_t(\theta_2^t, \phi_2^t), \dots, a_t(\theta_L^t, \phi_L^t)]$ is \tilde{F}_{BB} a matrix with $L \times N_s$ and matrix of array response vectors $N_t \times L$ is.

TABLE I
 COMPARISON OF COMPLEXITY.

Algo...	Computational Complexity (μ s)
OMP Algo [1]	$O(N_t^2 N_{RF}^t N_S)$
Suggested Algorithm	$O(N_t N_{RF}^t N_S^2)$

To determine the optimum values of precoders through D_t and \tilde{F}_{BB} .

Algorithm 1 : hybrid precoding scheme design based on GTD

Require: F_{opt}

1: $F_{RF} =$ Blank Matrix

2: $F_{res} = F_{opt}$

3: **for** $i \leq N_{RF}^t$ **do**

4: $\varphi = D_t^* F_{res}$

5: $k = \arg \max_{l=1, \dots, N_{cl} N_{ray}} (\varphi \varphi^H)_{l,l}$

6: $F_{RF} = [F_{RF} | D_t^{(k)}]$

7: $F_{BB} = (F_{RF}^H F_{RF})^{-1} F_{RF}^H F_{opt}$

8: $F_{res} = \frac{F_{opt} - F_{RF} F_{BB}}{\|F_{opt} - F_{RF} F_{BB}\|_F}$

9: **end for**

10: **update** F_{BB} through GTD

11: $\mathbf{F}_{BB} = N_s \frac{F_{BB}}{\|F_{RF} F_{BB}\|_F}$

12: **return** F_{RF}, F_{BB}

Algorithm 1 shows the pseudo-code for the suggested hybrid precoding technique based on GTD and the $a_i(\phi_{il}^t, \theta_{il}^t)$ vector is primarily resolute. Then the hybrid precoder (F_{RF}) of the analog part is modernized calculated values. The least-square approach is applied to the F_{BB} once all elements of the analog precoder section have been calculated. The whole beamforming vectors N_{RF}^t process is maintained has been chosen. The subsequent steps (Steps 11 and 10) are responsible for establishing the F_{BB} and enforcing the transmit power constraint using the GTD approach.

B. Computational Complexity Analysis

In [1], thoroughly investigated the difficulty of developing a hybrid precoding matrix based on the OMP algorithm is compared. It is essentially divided into 2 stages: the 1st is to design the original RF precoding and the computational complexity is $O(N_t N_S)$. The primary precoding matrix is modernized in the 2nd. After that, the residual matrix digital and analog precoding matrix layouts are created, which is similar to the OMP-based algorithm, and the complexity is $O(N_t N_{RF}^t N_S)$ and $O(N_t N_{RF}^t N_S)$, respectively. The next step involves processing the residual matrix to create an RF precoding vector n. Its complexity is $O(N_t N_{RF} N_S^2)$. Combining these two stages, when these two processes are combined, the proposed GTD precoding method complexity is $O(N_t N_{RF}^t N_S^2)$. For research and comparison, suppose the number of elements in the vector set in the OMP method is N_t . Therefore, the proposed GTD precoding complexity is less than the hybrid precoding technology created on the OMP algorithm. The complexity of the algorithm is shown in Table I.

VI. SIMULATION RESULTS

The Algorithm that has been proposed is as follows: In mmWave large MIMO systems, one section compares the simulation results of OMP-constructed hybrid precoding with analog, digital hybrid precoding. The simulation parameters we used in MATLAB R2021a are listed in Table II, and the results were averaged over 500 random channel implementations.

 TABLE II
 SIMULATION OF DIFFERENT PARAMETERS.

Parameters	Value
No. of clusters N_{cl}	8
No. of propagation paths/cluster N_{ray}	10
Antenna array deployed	ULA
AoA and AoD Uniform cluster angles distribution	$[0, 2\pi]$
Angular spread	7.5°
No. of Txr. antennas N_t	256
No. of Rxr. antennas N_r	64
SNR	10dB
No. of RF chains	4&6

Fig. 2. depicts the relationship between spectral efficiency (SE) and signal to noise ratio (SNR) for several precoding techniques with $N_t = 256$ and $N_r = 64$ antennas at the transmitter and receiver, with $N_{RF}^t = N_{RF}^r = 4$ RF chains and $N_{RF}^t = N_{RF}^r = [1, 2]$ using SVD and GTD decomposition algorithms respectively. That the increases SNR, The SE of various precoding techniques improved to varying degrees as the data streams grew larger.

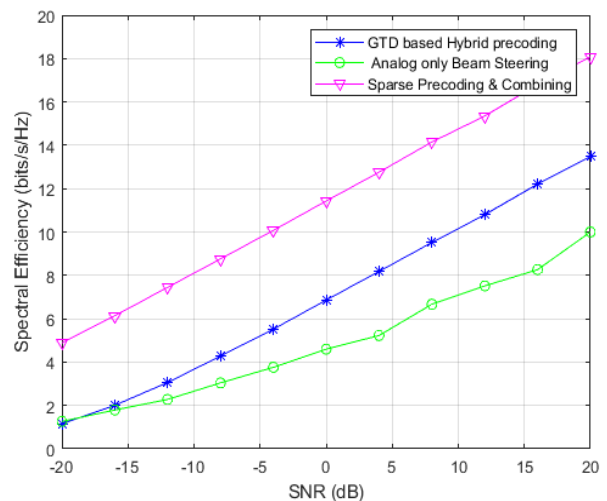


Fig. 2. SE versus SNR for GTD based Hybrid Precoding in a 256×64 system with 4 RF chains

The hybrid precoding scheme in terms of the SE performances is based on GTD proposed. In the performed simulation studies, That the data streams, N_S are assumed to be transmitted from a receiver with $N_r = 64$ antennas to a transmitter equipped with $N_t = 256$ antennas. The antennas for the receiver and transmitter antennas are designed as ULAs with $d = \lambda/2$. In addition, The configurations of $N_S = N_{RF}^t = N_{RF}^r = 2$ and $N_S = N_{RF}^t = N_{RF}^r = 6$ are two separate mmWave mMIMO systems, respectively, the simulation results are obtained to presented in Figure 2. In Section II the channel model is explained by the channel matrix is generated, the AoD and AoA are meant to follow a uniform distribution Within $[0, 2\pi]$. Moreover, in the 1st simulation, the number of propagation scattering routes is set to $L=2$, while in the 2nd simulation, it is set to $L=4$. Finally, random channel realizations 500 are used to produce simulation results.

The examine where the number of data streams is identical to the number of RF chains, i.e., $N_S = N_{RF}^t = N_{RF}^r = 2$ is in the 1st simulation. This statement is followed in the poorest case since the number of data streams can't be greater than the number of RF

chains according to $N_S \leq N_t^{RF} \leq N_t$ and $N_S \leq N_r^{RF} \leq N_r$ constraints. When the obtained results by comparing to the standard OMP algorithm scheme using GTD, it is obvious to provide enhanced for all SNR values even in the poorest situations in the proposed design.

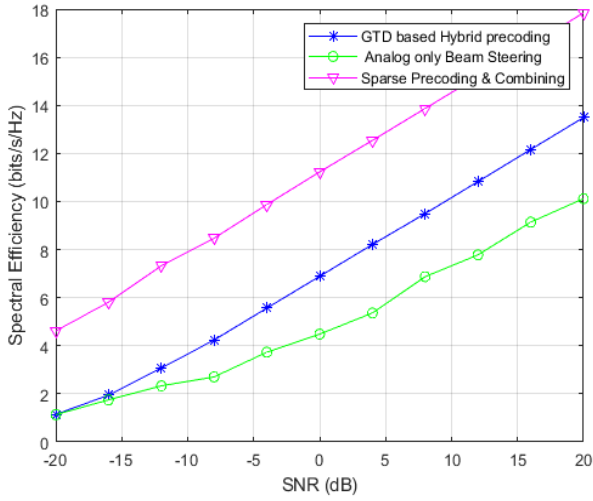


Fig. 3. SE versus SNR for GTD based Hybrid Precoding in a 256×64 system with 6 RF chains

The evaluated when the number of data streams is less than the number of RF orders that guarantee conditions $2N_S \leq N_{RF}^t$ and $2N_S \leq N_{RF}^r$ in the second simulation. Fig. 3. shows the SE obtained in the system with square planar arrays at receiver and transmitter in a 256×64 . The receiver and transmitter are supposed to have 4 transceiver chains that transmit $N_S = 1$ or 2 streams for the suggested precoding approach. Fig.3. shows the proposed framework achieves a SE that is equivalent to that obtained by the optimal solution without constraints on $N_S = 2$, deceits at a little deviation from the optimal on $N_S = 1$. The proposed strategy makes it possible to estimate very precisely the foremost singular vectors of the channel which are four director vectors. Traditional beam orientation as compared, Fig.3. shows the mmWave systems there is an excessive improvement over more complex precoding strategies with actual expire sizes.

Fig.4. shows the SE obtained the 256×64 with square planar arrays in both the receiver and the transmitter. Fig.4. shows the performance gain in a 256×64 system with $N_S = 1$ or 2 streams, $N_t^{RF} = N_r^{RF} = 4$ RF sequences. Fig.4. shows in the $N_S = 1$, that the SE realized by the proposed framework is equal to the spectrum efficiency obtained by the optimal solution without restrictions, and the difference between the spectrum efficiency and the efficiency of the spectrum obtained is very small. It is better when $N_S = 2$. That the proposed stratagem can very perfectly estimate the singular channel dominance vector as an arrangement of four control vectors. Compared with beam steering, Fig.4. shows in a millimeter-wave system with a convenient array size, the more complex encryption strategy has been significantly improved. To explore the performance of a millimeter-wave system with a longer antenna range, Fig.5. plots a 256×64 system as $N_t^{RF} = N_r^{RF} = 6$ radio frequency strings are the performance achieved and the $N_S = 1$ and $N_S = 2$ are the proposed method almost performance achieved.

The proposed agenda exploits the mathematical structure of huge mmWave channels through comparatively partial diffusion. Towards

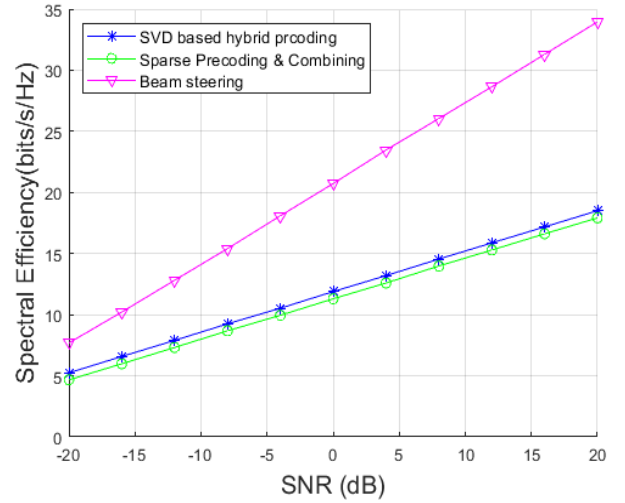


Fig. 4. SE versus SNR for SVD based Hybrid Precoding in a 256×64 system with 4 RF chains

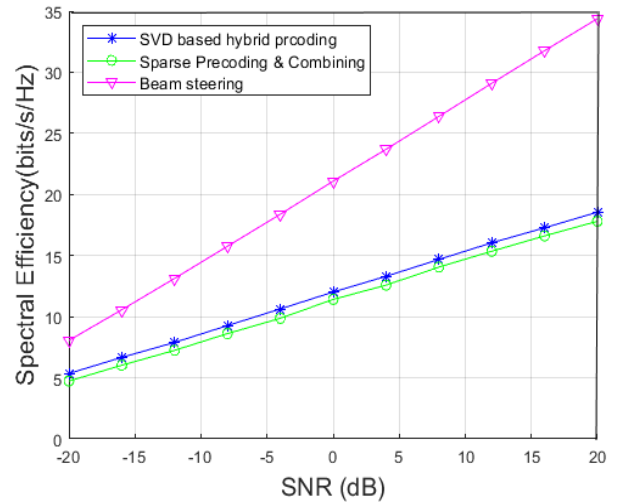


Fig. 5. SE versus SNR for SVD based Hybrid Precoding in a 256×64 system with 6 RF chains.

test show in a propagation medium with different scattering stages, Fig.6. plots the SE as a function of the angular spread of the channel for several mmWave system alignments. Fig.6. shows that when the angular difference is small. As the angle difference increase, the rate of gain of the proposed solutions will gradually decrease. However, Fig.5. shows that in the two cases $N_S = 1$ presented, the exchange rate difference is still less than 10% at the angular difference of 15° is significant and is slight for a more sensible angle difference is approximately 5° . This $N_t^{RF} = N_r^{RF} = 4$ and $N_S = 2$ with 256×64 system is seen by examining. If conceivable, Observing the same 256×64 system with $N_t^{RF} = N_r^{RF} = 6$ demonstrates this.

VII. CONCLUSION

To prevent the complicated bit allocation in the standard SVD-constructed hybrid precoding by using GTD-based hybrid precoding. With the use of GTD, we discovered that the mmWave MIMO channel may be split into many sub-channels with similar SNRs, preventing the need for sophisticated bit allocation. We've also recommended designing digital and analog precoders, with the

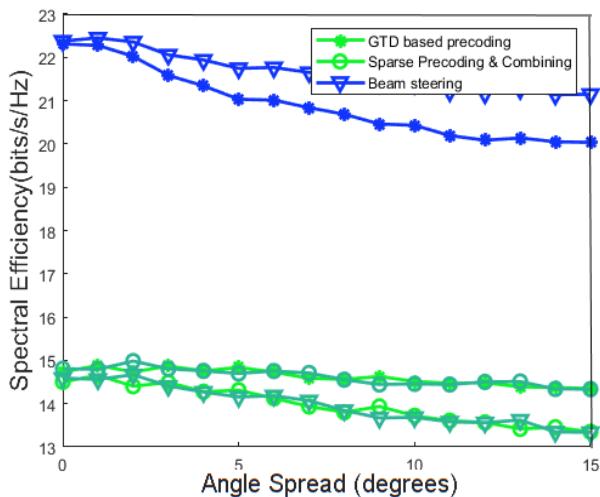


Fig. 6. SE VS AS in different mmWave system formation at an SNR of 0dB

digital precoder being formed using GMD and the analog precoder being created using the basis pursuit principle. The suggested GTD-based hybrid precoding achieves greater performance than the typical SVD-based hybrid precoding, according to simulation results.

REFERENCES

- [1] El Ayach, Omar, et al. "Spatially sparse precoding in millimeter wave MIMO systems." *IEEE TRANSACTIONS ON WIRELESS COMMUNICATIONS*, VOL. 13, NO. 3, MARCH 2014 <http://doi.org/10.1109/TWC.2014.011714.130846>.
- [2] Zhang, Dan, et al. "SVD-based low-complexity hybrid precoding for millimeter-wave MIMO systems." *IEEE Communications Letters* 22.10 (2018): pp.2176-2179. <http://doi.org/10.1109/LCOMM.2018.2865731>.
- [3] F. Zhang and M. Wu, "Hybrid analog-digital precoding for millimeter wave MIMO Systems," in 2017 IEEE 17th International Conference on Communication Technology (ICCT), Chengdu, China, aug 2017. <http://doi.org/10.1155/2021/5532939>.
- [4] X. Liu, X. Li, S. Cao, et al., "Hybrid precoding for massive mmWave MIMO systems," *IEEE Access*, vol. 7, pp. 33577–33586, 2019.
- [5] E. Zhang and C. Huang, "On achieving an optimal rate of digital precoder by RF-baseband codesign for MIMO systems," in Proc. 80th IEEE Veh. Technol. Conf. (VTC Fall), Vancouver, BC, Sept. 2014, pp. 1–5. <https://doi.org/10.1109/VTCFall.2014.6966076>.
- [6] F. Sotrabadi and W. Yu, "Hybrid digital and analog beamforming design for large-scale antenna arrays," *IEEE J. Sel. Topics Signal Process.*, vol. 10, no. 3, pp. 501–513, Apr. 2016. <https://doi.org/10.1109/JSTSP.2016.2520912>.
- [7] C. Rusu, R. Mèndez-Rial, N. González-Prelcic, and R. W. Heath, "Low complexity hybrid precoding strategies for millimeter-wave communication systems," *IEEE Trans. Wireless Commun.*, vol. 15, no. 12, pp. 8380–8393, Dec. 2016. <http://doi.org/10.1109/TWC.2016.2614495>.
- [8] R. Rajashekar and L. Hanzo, "Hybrid beamforming in mm-wave MIMO systems having a finite input alphabet," *IEEE Trans. Commun.*, vol. 64, no. 8, pp. 3337–3349, Aug. 2016. <http://doi.org/10.1109/TCOMM.2016.2580671>.
- [9] Zhang, Didi, et al. "Hybridly connected structure for hybrid beamforming in mmWave massive MIMO systems." *IEEE Transactions on Communications* 66.2 (2017): 662-674. <http://doi.org/10.1109/TCOMM.2017.2756882>.
- [10] Lu, Yiqi, et al. "Improved hybrid precoding scheme for mmWave large-scale MIMO systems." *IEEE Access* 7 (2019): 12027-12034. <http://doi.org/10.1109/ACCESS.2019.2892136>.
- [11] Jindal, Nihar. "MIMO broadcast channels with finite-rate feedback." *IEEE Transactions on information theory* 52.11 (2006): 5045-5060. <http://doi.org/10.1109/TIT.2006.883550>.
- [12] Rusek, Fredrik, et al. "Scaling up MIMO: Opportunities and challenges with very large arrays." *IEEE signal processing magazine* 30.1 (2012): 40-60. <http://doi.org/10.1109/MSP.2011.2178495>.
- [13] A. S. Lewis and J. Malick, "Alternating projections on manifolds," *Mathematics of Operations Research*, vol. 33, no. 1, pp. 216–234, 2008.
- [14] R. Escalante and M. Raydan, *Alternating Projection Methods*. Society for Industrial and Applied Mathematics, 2011, vol. 8. <https://doi.org/10.1137/9781611971941>.
- [15] Y. Jiang, W. Hager, and J. Li, "The generalized triangular decomposition," *Mathematics of computation*, vol. 77, no. 262, pp. 1037–1056, 2008.
- [16] C. Weng, C.-Y. Chen, and P. Vaidyanathan, "Generalized triangular decomposition in transform coding," *IEEE transactions on signal processing*, vol. 58, no. 2, pp. 566–574, 2009. <http://doi.org/10.1109/TSP.2009.2031733>.
- [17] Y. Kabalci and H. Arslan, "Hybrid precoding for mm-wave massive MIMO systems with generalized triangular decomposition," 2018 IEEE 19th Wireless and Microwave Technology Conference (WAMICON), pp. 1–6, 2018.
- [18] M. Su, Y. Huang, C. Zhang, J. Zhang, and Y. Li, "Hybrid Precoder Design for Millimeter Wave Systems Based on Geometric Construction," 2017, pp. 1–6. <https://doi.org/10.1109/GLOCOM.2017.8254858>.
- [19] M. Xiao et al., "Millimeter-Wave Communications for Future Mobile Networks," *IEEE J. Sel. Areas Commun.*, vol. 35, no. 9, pp. 1909–1935, Sep. 2017. <https://doi.org/10.1109/JSAC.2017.2719924>.
- [20] W. Yuan, V. Kalokidou, S. M. D. Armour, A. Doufexi, and M. A. Beach, "Application of Non-Orthogonal Multiplexing to mmWave Multi-User Systems," 2017, pp. 1–6.
- [21] S. Yong and C. Chong, "An overview of multigigabit wireless through millimeter wave technology: potentials and technical challenges," *EURASIP J. Wireless Commun. Netw.*, vol. 2007, no. 1, pp. 50–50, 2007. <https://doi.org/10.1155/2007/78907>.
- [22] R. Daniels and R. W. Heath, Jr., "60 GHz wireless communications: emerging requirements and design recommendations," *IEEE Veh. Technol. Mag.*, vol. 2, no. 3, pp. 41–50, 2007. <http://doi.org/10.1109/MVT.2008.915320>.